JPE 3-2-4

High Performance Adjustable-Speed Induction Motor Drive System Incorporating Sensorless Vector Controlled PWM Inverter with Auto-Tuning Machine-Operated Parameter Estimation Schemes

[1]Koji Soshin*, [2]Yukihiko Okamura, [3]Tarek Ahmed and [4]Mutsuo Nakaoka

[1,2]Sensing & Communication Technology Research & Development Laboratory Matsushita Electric Works, Ltd., 1048 Kadoma, Osaka 571-8686, Japan

[3,4]Dept. of Electrical and Electronics Eng., Yamaguchi University, Yamaguchi, 755-8611, Japan

ABSTRACT

This paper presents a feasible development on a highly accurate quick response adjustable speed drive implementation for general purpose induction motor which operates on the basis of sensorless slip frequency type vector controlled sine-wave PWM inverter with an automatic tuning machine parameter estimation schemes. In the first place, the sensorless vector control theory on the three-phase voltage source-fed inverter induction motor drive system is developed in slip frequency based vector control principle. In particular, the essential procedure and considerations to measure and estimate the exact stator and rotor circuit parameters of general purpose induction motor are discussed under its operating conditions. The speed regulation characteristics of induction motor operated by the three-phase voltage-fed type current controlled PWM inverter using IGBT's is illustrated and evaluated for machine parameter variations under the actual conditions of low frequency and high frequency operations for the load torque. In the second place, the variable speed induction motor drive system, employing sensorless vector control scheme which is based on three-phase high frequency carrier PWM inverter with automatic tuning estimation schemes of the temperature-dependent and -independent machine circuit parameters, is practically implemented using DSP-based controller. Finally, the dynamic speed response performances for largely changed load torque disturbances as well as steady state speed vs. torque characteristics of this induction motor control implementation are illustrated and discussed from an experimental point of view.

Keywords: Induction Motor, Sesorless Vector Control, Sine-wave PWM Inverter, IGBT

1. Introduction

In recent years, a variety of advanced power electronics control and systems integration technologies relating to the high performance adjustable-speed drives for induction motor applications which are based on the voltage-source type three-phase current controlled PWM inverter using IGBTs and its associated vector control scheme have attracted special interest in the fields of the industrial, transportation and consumer AC motor drives as well as electric vehicle AC motor drives. Thus, the exact stator and rotor circuit

Manuscript received Dec. 18, 2002; revised April 1, 2003.
Corresponding Author: soushin@hkrl.mew.co.jp
Tel : +81-6-6906-3471, Fax : +81-6-6906-0772

parameters of general purpose induction motors operated different types under various load operating conditions should be measured and estimated automatically for the purpose of sensorless vector control implementation introduced for the induction motor variable-speed drives.

In particular, the complex temperature-dependent rotor resistance variations of application specific types of induction motor and different type induction motors are actually more significant in not only the steady state speed regulation accuracy but also for the settling time at the transient speed responses. It is difficult to achieve the sufficient speed regulation accuracy in steady state as well as the speed settling time in dynamic state which are required for wide speed setting ranges and largely changed load torque disturbances. In order to solve these feasible problems mentioned above, the authors have developed a simple and practical automatic auto-tuning method to measure and estimate the exact stator and rotor circuit parameters of application specific induction motors addition to some different types of general purpose induction motors used from diverse application viewpoints.

In addition to these, the high performance induction motor variable speed drives employing sensorless vector control based on three-phase PWM inverter with a specific automatic auto-tuning machine parameter estimation scheme which is introduced to transient torque current component due to transient current suppression.

This paper presents the state-of-the-art feasible development and characterization on the general purpose and application specific induction motor variable speed drives in industry which applies for sensorless slip-frequency-based vector control implementation with a novel automatic auto-tuning machine operated parameter estimation scheme. The experimental results in the feasible induction motor drive system treated here are illustrated for speed regulation characteristics in steady state in addition to speed setting performances in dynamic state and discussed from a practical point of view.

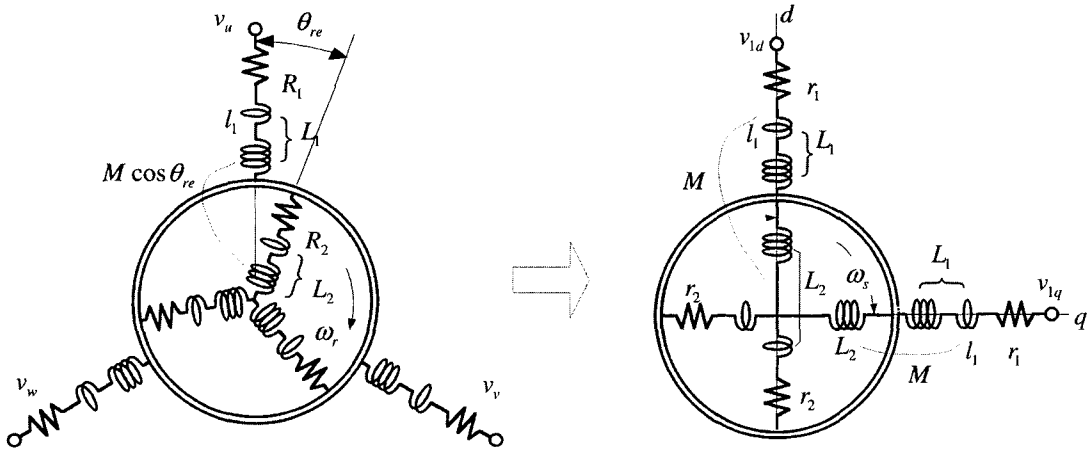

Fig. 1. Equivalent dynamic circuit of induction motor on plane transformed to d-q coordinate frame axis.

r_1 : Stator winding resistance

r_2 : Rotor equivalent resistance

L_1 : Stator winding inductance

L_2 : Rotor equivalent inductance

l_1 : Stator leakage inductance

l_2 : Rotor leakage inductance

i_{1d} : d-axis exiting current component

i_{1q} : q-axis torque current component

v_{1d} : d-axis input voltage

v_{1q} : q-axis input voltage

M : Mutual inductance between L_1 - L_2

ω_s : Slip angular frequency

ω : Rotor angular speed of d-q axis

ω_r : Rotor speed of 3-phase dynamic model

2. System Description and Control Strastage

As shown in Fig. 1, in order to perform the speed sensorless vector control of the induction motor, 2-axis model which carried out coordinates conversion at the synchronous rotation rectangular coordinates system (d-q coordinates) which rotates in the angular frequency of secondary magnetic flux from the equal circuit expressed with 3 phase AC will be treated in this paper.

Fig. 2 shows an adjustable-speed induction motor drive system using slip frequency mode vector control based on three-phase PWM inverter using the latest IGBTs. This induction motor variable speed drive system incorporates PI control strategy to delay the torque current component in order to suppress the transient current over under largely changed load conditions. In Fig. 2 ϕ equals to $L_1 i_{1d}$.

Equation (1) gives the general voltage equation of induction motor described and formulated on rectangular coordinates (d-q frame coordinates), in which rotation angle frequency denoted as ω.

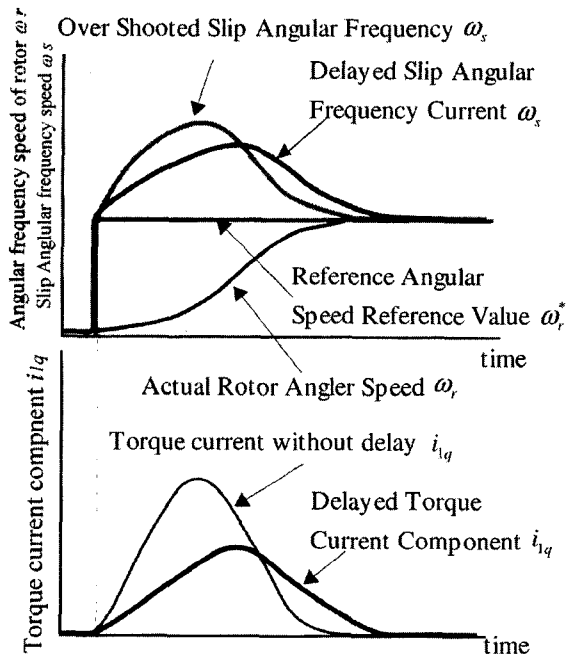

Fig. 2. Influence on transient mode of in the case of increasing torque current component.

$$\begin{bmatrix} v_{1d} \\ v_{1q} \\ 0 \\ 0 \end{bmatrix} = \begin{bmatrix} r_1 + \sigma L_1 p & -\sigma L_1 \omega & (M/L_2)p & -(M/L_2)\omega \\ \sigma L_1 \omega & r_1 + \sigma L_1 p & (M/L_2)\omega & (M/L_2)p \\ -Mr_2/L_2 & 0 & r_2/L_2 + p & -\omega_s \\ 0 & -Mr_2/L_2 & \omega_s & r_2/L_2 + p \end{bmatrix} \begin{bmatrix} i_{1d} \\ i_{1q} \\ \phi_{2d} \\ \phi_{2q} \end{bmatrix} \quad (1)$$

where, i_{1d} : Exiting current component of d-axis

i_{1q} : Torque current component of q-axis

L_1 : Stator winding inductance

L_2 : Rotor equivalent inductance

r_1 : Stator winding resistance

r_2 : Rotor equivalent resistance

p : Differential operator ($=d/dt$)

ω : Rotor angular speed

ω_s : Slip angular frequency

σ : Leakage flux coefficient ($=1-M^2/L_1L_2$)

M : Mutual inductance between stator winding inductance L_1 and cage form rotor inductance L_2

v_{1d} : Input voltage of d-axis

v_{1d}^* : Initial voltage vale of d d-axis

v_{1q} : Input voltage of q-axis

ϕ_{2d}, ϕ_{2q} : d-axis and q-axis components of rotor flux described by

$$\phi_{2d} = Mi_{1d} + L_2 i_{2d} \qquad \phi_{2q} = Mi_{1q} + L_2 i_{2q} \quad (2)$$

Equation (3) is a state-space vector equation estimated by rewriting equation (1).

$$P\begin{bmatrix} \sigma L_1 i_{1d} \\ \sigma L_1 i_{1q} \\ \phi_{2d} \\ \phi_{2q} \end{bmatrix} = \begin{bmatrix} -r_1 - (M/L_2)^2 r_2 & \sigma L_1 \omega & (Mr_2/L_2)^2 & (M/L_2)\omega_r \\ \sigma L_1 \omega & -r_1 - (M/L_2)^2 r_2 & -(M/L_2)\omega_r & (M/L_2)^2 \\ Mr_2/L_2 & 0 & -r_2/L_2 & \omega_s \\ 0 & Mr_2/L_2 & -\omega_s & r_2/L_2 \end{bmatrix} \begin{bmatrix} i_{1d} \\ i_{1q} \\ \phi_{2d} \\ \phi_{2q} \end{bmatrix} + \begin{bmatrix} v_{1d} \\ v_{1q} \\ 0 \\ 0 \end{bmatrix} \quad (3)$$

Torque of the induction motor T_e is expressed as equation (4) with the sum and products style of rotor flux and stator current.

$$\begin{aligned} T_e &= pM(i_{1q} \cdot i_{2d} - i_{1d} \cdot i_{2q}) \\ &= p\frac{M}{L_2}(i_{1q}\phi_{2d} - i_{1d}\phi_{2q}) \end{aligned} \quad (4)$$

i_{1d} : d-axis current component of the stator winding

i_{1q} : q-axis current component of the stator windings

i_{2d} : d-axis current component of the rotor

i_{2q} : d-axis current component of the rotor

ϕ_{2d} : d-axis number of magnetic-flux interlinkage of the rotor

ϕ_{2q} : q-axis number of magnetic-flux interlinkage of the rotor

In the equation (4), torque T_e will be able to controlled very easy by controlling the rotor magnetic flux ϕ_{2q} to keep certain value and controlling the rotor magnetic flux in order to be proportional to the current orthogonalizes to rotor magnetic flux ϕ_{2q}.

Rotator interlinkage magnetic flux ϕ_{2d} equal to Mi_{1d} and $\phi_{2q} = 0$ as shown in equation (5), it is possible to control torque T_e linearly just like the DC motor.

$$\phi_{2d} = Mi_{1d} \text{ (constant)}, \quad \phi_{2q} = 0 \tag{5}$$

The torque of T_e shown in equation (4) is expressed as following equation (6) under the conditions of equation (5)

$$T_e = p\frac{M}{L_2}\phi_{2d} \cdot i_{1q} \tag{6}$$

If the conditions of equation (6) is satisfied, reference value ω_s of slip angular frequency can be formulated by the equation (7).

$$\omega_s = \frac{r_2 M}{L_2 \phi_{2d}} i_{1q} \approx \frac{r_2}{\phi_{2d}} i_{1q} = K_m i_{1q} \tag{7}$$

K_m in equation (7) is the gain of slip angular frequency ω_s, and is given by the following equation (8).

$$K_m = \frac{r_2}{\phi_{2d}} \tag{8}$$

Vector controlled PWM inverter supplies the specific voltage expressed by equation (9) substituting $\phi_{2d} = Mi_{1d}$ (constant) and $\phi_{2q} = 0$ to equation (1) for the induction motor in steady state.

$$\begin{bmatrix} v_{1d} \\ v_{1q} \end{bmatrix} = \begin{bmatrix} r_1 & -\sigma L_{1d} \\ L_1\omega & r_1 \end{bmatrix} \begin{bmatrix} i_{1d} \\ i_{1q} \end{bmatrix} \tag{9}$$

Under these conditions, ω_s is calculated from the torque current components i_{1q} by rewriting equation (3) and the velocity of induction motor could be coincided with the reference value of the stator frequency adding ω_s^* to speed reference ω_r^*.

In a transient condition, the slip angular frequency ω_s is formulated by equation (10) on the basis of substituting equation (9) to equation (3). As a result, ω_s can be obtained by

$$\omega_s = \frac{r_2 M}{L_2 \phi_{2d}} i_{1q} + \frac{\sigma L_1 M}{L_2 \phi_{2d}} p i_{1q} \tag{10}$$

According to equation (10), not only proportional term of torque current component i_{1q} but also differential term of torque current component i_{1q} will be influenced to ω_s. Then calculated reference value of stator frequency ω can be larger by differential term. Therefore, it will be difficult to realize stable speed-adjustment in accordance with increasing of the slip frequency ω_s. The motor shaft speed ω can be regulated by not making drastic changes of the reference slip frequency ω_s^*. The reference slip frequency ω_s^* is calculated by substituting the output value of the PI controller which input is the detected torque current component i_{1q}, as indicated in equation (10) above.

Because the inverter provides the voltage compensated for the voltage drop which is caused by the motor. If the starter resistance r_1 and the inductance L_1 value set to the inverter have some error with the actual value of r_1 and L_1, the error appears as the error of motor current.

On the other hand, the rotor resistance r_2 is to be contained in the proportional coefficient for operating slip angular frequency from torque current component in

equation (10), the error of rotor resistance r_2 is to cause an error of slip angular frequency ω_s.

The effect of the integrator adopted in order to negate the influence of the slip angular frequency ω_s by this differential coefficient of equation (10) is shown in Fig. 2. Fig. 2 shows the difference between the case where detected torque current component i_{1q} is directly used as slip angular-frequency reference value i_{1q}, and the case where detected torque current component i_{1q} is delayed by the integrator. Since large overshoot appears in slip angular frequency ω_s in case where there is no integrator. Fig. 2 shows that it is the validity of an integrator.

3. Novel Practical Approach of Machine Parameters

3.1 Influence of the induction motor parameter errors

In this section, the novel automatic auto-tuning scheme of the induction motor parameters is that is necessary to be driven by vector controlled inverter is explained. Fig. 3 depicts the developed dynamic model of the senseless vector controlled PWM inverter system. This system is designed as follows.

Detecting the stator current by the current sensor, carries out vector control operation by the microprocessor based on that stator current value, calculates the voltage reference value for obtaining instant torque component

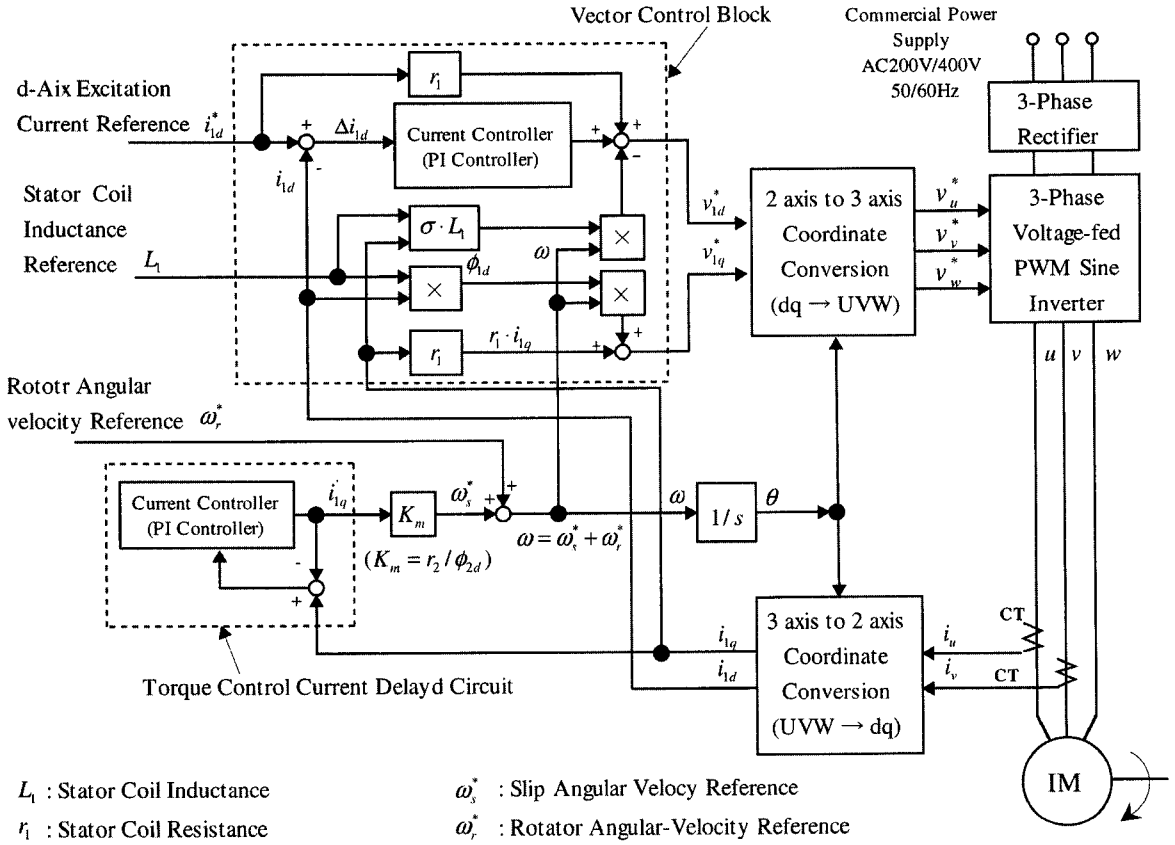

L_1 : Stator Coil Inductance
r_1 : Stator Coil Resistance
σ : Leakage Flux Coefficient
θ : electrical angle for Axis-of-coordinates conversion / reverse conversion
ω_s^* : Slip Angular Velocy Reference
ω_r^* : Rotator Angular-Velocity Reference
ω : Voltage Angular Frequency $(\omega = \omega_s^* + \omega_r^*)$

Fig. 3. Schematic block diagram of sensorless vector controlled inverter system for induction motor drive.

current i_{1q} and the voltage reference value is given to a 3 phase-voltage type PWM inverter as a result. The vector control operation needs some motor parameters. They are following four parameters.

L_1 : Stator winding inductance

l_2 : Leakage inductance

r_1 : Stator winding

r_2 : Rotator equivalent resistance

Fig. 4 represents the experimental result of the induction motor speed regulation under the conditions of low frequency at 3Hz and high frequency at 60Hz in case of adapting some errors to three motor parameters. Fig. 4-(a) shows that stator winding resistance r_1 influences the speed regulation in the range of low frequency, and also stator winding inductance L_1 influences the speed regulation in the range of high frequency. Fig. 4-(b) displays the rotor resistance r_2 gives influence to the speed regulation for any frequency range. Fig. 4-(c) displays that the error of stator winding inductance L_1 has large influence in higher frequency (60Hz). Fig. 4-(d) shows that the leakage inductance l_2 does not give much influence. The above result shows as follows.

When the general-purpose induction motor is driven by the vector control inverter system, if the parameters of stator winding resistance r_1, stator winding inductance L_1 and rotator equivalent resistance r_2 can be estimated, it is possible to control the three phase induction motor with sufficient accuracy. However, it is difficult for user to estimate the parameters of the general-purpose induction

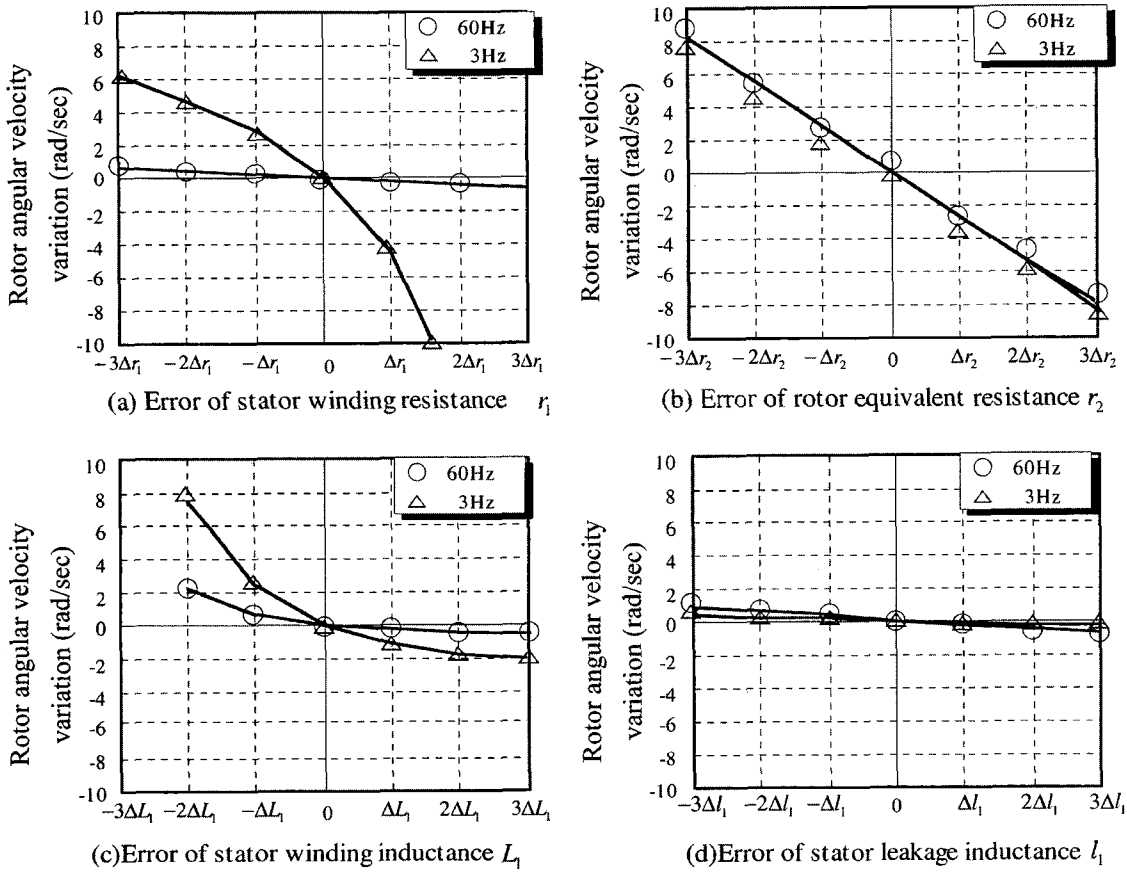

Fig. 4. Relationship between error of induction motor parameters and speed change.

motor in fact.

The reasons are

(1) User needs to input the parameters of the induction motor into the vector control inverter system.

(2) User needs the special measuring device and special technical knowledge to estimate the parameters of the induction motor.

Then, if the vector controlled inverter system itself can measure the parameters of the adapted general purpose induction motor, the optimal speed control and optimal torque control of the induction motor will become possible without a burden of a user and also flexibility will becomes very high.

Next, in order to judge the possibility of measurement of the induction motor circuit constants required for vector control inverter system, the relationship between the stator winding resistance r_1, rotator equivalent resistance r_2, stator winding inductance L_1, d-axis current component of the stator i_{1d}, q-axis current component of the stator i_{1q} and rotor angular speed ω_r of the induction motor parameter are measured.

Fig. 5 represents the experimental results of the rotor current regulation so as to adapt in accordance with some errors to three induction motor types of system circuit parameters. Fig. 5 (a) and 5 (c) show that the variations of the stator winding resistance r_1 and stator inductance L_1 cause the variation of stator current i_{1q} and i_{1d}.

Therefore, it is possible to estimate its stator winding resistance r_1 and stator winding inductance L_1 by measuring the stator current. But Fig. 5 (b) shows that the speed sensing operation should be necessary to measure the rotor speed of the motor ω_r itself because changing rotor resistance r_1 changes the rotor speed ω_r but not the stator current i_{1q} and i_{1d} does not change the rotor speed ω_r.

The novel automatic estimation scheme of these motor parameters without speed sensor is discussed below.

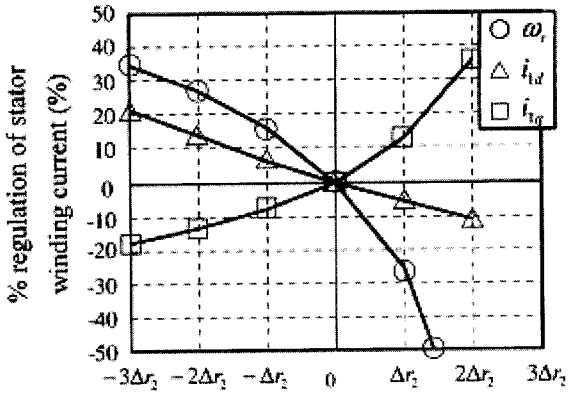

(a) Error of rotor winding resistance r_1

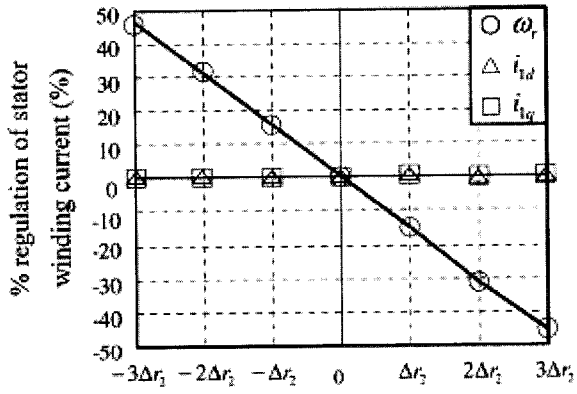

(b) Error of rotor equivalent resistance r_2

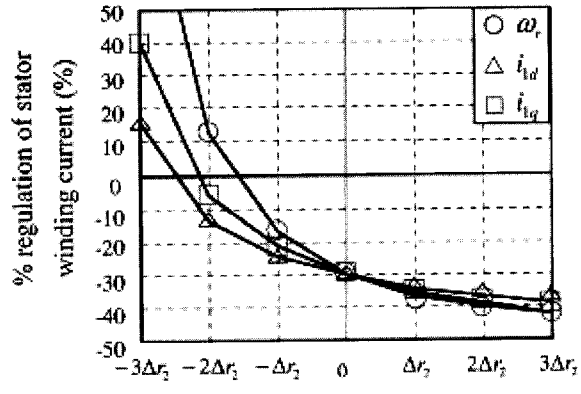

(c) Error of stator winding inductance L_1

Fig. 5. Relationship between error of induction motor parameters and speed variation.

3.2 Estimation of stator resistance

The rotor winding resistance r_1 of the induction motor should be estimated when this motor does not rotate to avoid the influence of the stator inductance L_1. Under

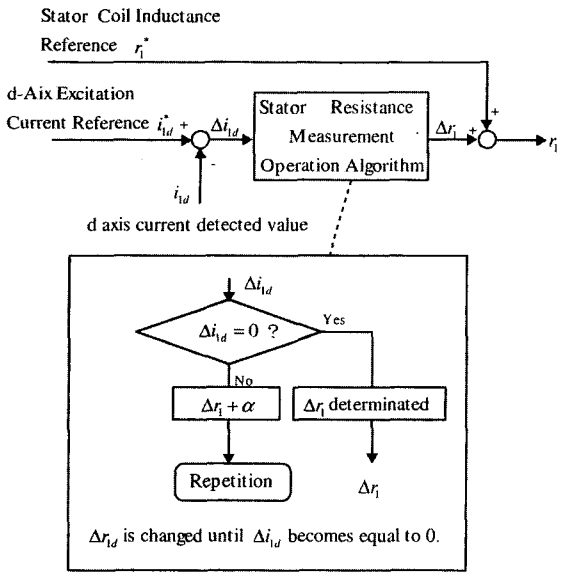

Fig. 6. Schematic block diagram to estimate the resistance of induction motor stator.

this condition, the induction motor does not generate the output torque at all, then the torque current component i_{1q} is equal to zero, thus the following equation described as the product of r_1 and i_{1d}^* can be obtained by substituting $v_{1q} = 0$ to equation of $v_{1d} = r_1 i_{1d}^*$.

Accordingly, adapting this initial value of v_{1d}^* to the motor, measuring actual exciting current i_{1d} and adjusting r_1 value in order that i_{1d} will be equal to i_{1d}^*. As a result, stator resistance r_1 can be estimated.

Fig. 6 shows the method to estimate the stator resistance r_1. This measuring apparatus consists of the integrator.

3.3 Estimation of stator inductance

After measuring the stator resistance r_1, the stator inductance L_1 is measured by driving the induction motor at constant speed with no-load. In this case, the deviation of angular velocity ω_s and the torque current component i_{1q} are zero. Substituting $i_{1q} = 0$ to the equation (9), the equation (9) can be rearranged to the following equations.

$$v_{1d} = r_1 \cdot i_{1d}^* \qquad (11) - (a)$$

$$v_{1q} = \omega \cdot \phi \qquad (11) - (b)$$

$$\phi = L_1 \cdot i_{1d}^* \qquad (11) - (c)$$

The reference flux ϕ determined by the rated voltage of the induction motor is described as the product of the stator inductance L_1 and the exciting current component i_{1d}.

That is,

$$i_{1d}^* = \phi / L_1 \qquad (12)$$

According to the equation (12), the mismatched error of stator inductance ΔL_1 is to be detected as a variation of the exciting current component i_{1d}. The staor inductance L_1 is measured by the following procedure. If the stator inductance is ΔL_1 larger than the preset value into the inverter, exciting current component i_{1d} is smaller as Δi_{1d}. For example, the value of an actual induction motor stator winding inductance L_1 is larger ΔL_1 more than above-mentioned initial-setting value L_1^*, from the equation of $i_{1d}^* = \phi / L_1$, d-axis current i_{1d} of excitation current component becomes more smaller than the actual value of i_{1d} and using the difference of Δi_{1d}, the equation of $i_{1d}^* = \phi / L_1$ will be an deform into the form equation (13).

$$i_{1d}^* + \Delta i_{1d} = \phi / (L_1 + \Delta L_1) \qquad (13)$$

Equation (14) is obtained by subtracting equation (12) from equation (13).

$$\Delta i_{1d} = \left[\frac{1}{(L_1 + \Delta L_1)} - \frac{1}{L_1} \right] \cdot \phi \qquad (14)$$

Reference voltage v_{1q} of q-axis is obtained by the equation (11)-(b). The rotation speed of the induction motor is constant, since interlinkage magnetic-flux ϕ is the constant and change of d-axis current i_{1d} of a stator winding does not affect q-axis reference voltage v_{1q}^*.

However, since d-axis voltage v_{1d} of the stator winding is influenced by the error of d-axis current i_{1d} from the equation (11)-(a) and the error of stator winding inductance L_1 is influenced as a result, and it can express with the equation (15).

$$\Delta v_{1d} = r_1 \cdot \Delta i_{1d} = \left[\frac{1}{(L_1 + \Delta L_1)} - \frac{1}{L_1}\right] \cdot r_1 \cdot \phi \qquad (15)$$

Since the stator winding resistance r_1 has been measured and fixed, the difference between the reference value and the detected value of exciting current component Δi_{1d} depends on the mismatched error of the stator inductance. Therefore, by adjusting the reference value of the exciting current component i_{1d}^{*} as to be the same as the detected exciting current component i_{1d}, the stator inductance will be exactly set to the actual value.

The stator inductance estimation system is demonstrated in Fig. 7.

In Fig. 7, i_{1d}^{**} is the preset value of reference exciting current component.

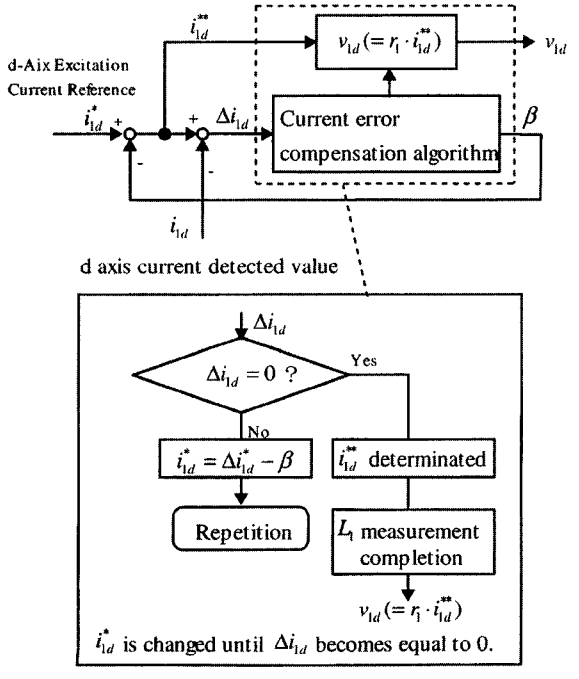

Fig. 7. Schematic block diagram of inductance detector of induction motor stator winding.

3.4 Estimation of rotor resistance

When the terminals of the induction motor driven by the sine-wave PWM inverter are opened, the motor terminal voltage v_a will decreases gradually shown in Fig. 8.

This voltage v_a is defined as the residual voltage, and represented by equation (16).

$$v_a = -\sqrt{2}\omega_r M \cdot I_{20} e^{-t/\tau_0} \cdot \sin(\omega_r t + \theta_0) \qquad (16)$$

where, M : Mutual inductance between stator winding inductance L_1 and rotator inductance L_2

v_a : Voltage value in real-time t of the residual-voltage damped-wave

ω_r : Rotation angular velocity of the induction motor

I_{20} : Actual rotator current value which flows just before the power supply terminal of the induction motor is opening

τ_0 : Damping time constant $(\tau_0 = L_2 / r_2)$ (17)

θ_0 : Phase angle

The damping performance of the residual voltage is determined by the damping time constant T_0 and the motor speed ω_r, and its frequency is equal to the motor speed.

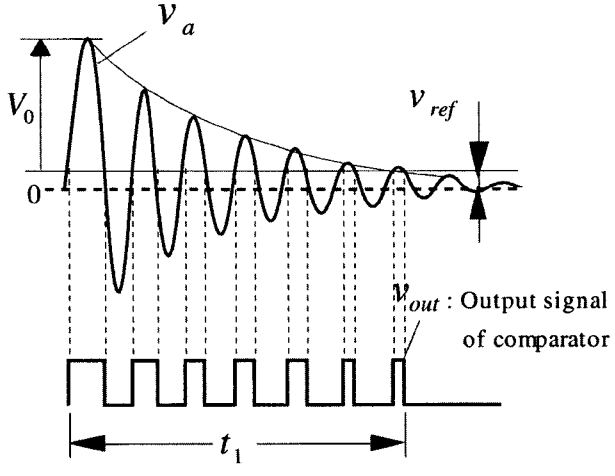

Fig. 8. Relationship between Residual voltage and output voltage of the comparator.

The damping time constant τ_0 is constituted of the rotor resistance r_2 and the rotor inductance L_2 ($\tau_0 = L_2/r_2$). Therefore, the rotor resistance r_2 can be calculated from the damping time constant T_0 which is determined by the motor terminal voltage.

Fig. 9 illustrates the relationship between the residual voltage and the output voltage of its detecting circuit.

Fig. 9 also indicates the schematic block diagram of the processing circuit to detect the residual voltage v_a. The detecting circuit of the residual voltage constituted by the comparator and the photo-coupler, is very simple. When the residual voltage v_a is higher than the reference voltage v_{ref}, the frequency of output voltage V_0 of the measuring circuit corresponds to the frequency of the residual voltage. On the other hand, when the residual voltage v_a is lower than the reference voltage v_{ref}, the output voltage V_0 does not change any more.

As shown in Fig. 8 and Fig. 9, a novel estimation system of the rotor inductance L_2 will be explained in the following.

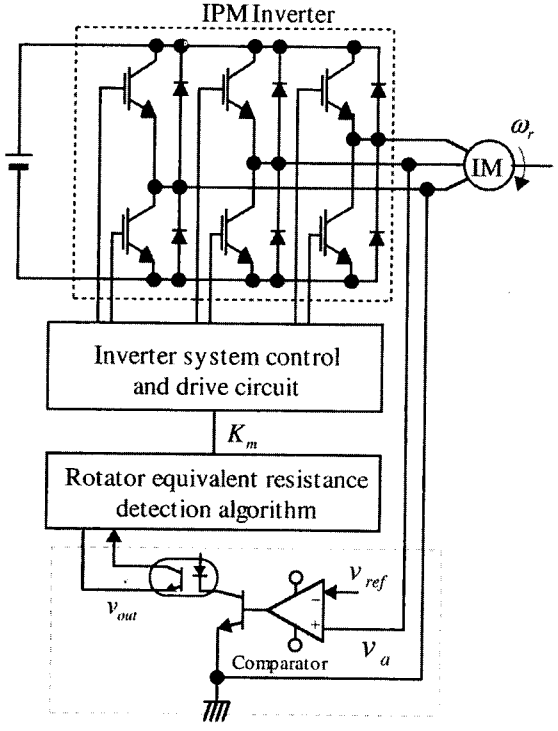

Fig. 9. Schematic block diagram of detecting residual voltage.

Under the no-load condition, the decreasing of the motor speed is too small and it can be ignored after opening the motor terminals.

Considering the amplitude of the residual voltage alone, the peak voltage value of the residual voltage v_a is defined as $V_0 = \left| -\sqrt{2}\omega_r M \cdot I_{20} \right|$, then equation (18) can be obtained.

$$v_a = V_0 \cdot e^{-t/\tau_0} \tag{18}$$

where, $V_0 = \left| -\sqrt{2}\omega_r M \cdot I_{20} \right|$

In Fig. 8, when t_1 which is the time for the residual-voltage v_a to decline and become criteria comparison voltage $v_{ref.}$ is substituted for equation (18), the following equation (19) will be obtained.

$$v_{ref.} = V_0 \cdot e^{-t_1/\tau_0} \tag{19}$$

This is transformed.

$$e^{-t_1/\tau_0} = v_{ref.}/V_0 \tag{20}$$

Calculating the logarithm of both the sides

$$-\frac{t_1}{\tau_0} = \ln\left(\frac{v_{ref.}}{V_0}\right) \tag{21}$$

Substituting equation (17) $\tau_0 = L_2/r_2$, $L_1 \cong L_2$ and equation (11)-(c) $\phi = L_1 \cdot i_{1d}$ into equation (20) and solves about r_2 then equation (22) will be obtained.

It will be clear that the rotator equivalent resistance r_2 can be observed from the following equation (22).

$$r_2 = \frac{L_2}{t_1}\ln\left(\frac{v_{ref.}}{V_0}\right) = \frac{\phi}{i_{1d} \cdot t_1}\ln\left(\frac{v_{ref.}}{V_0}\right) \tag{22}$$

Finally, the gain coefficient K_m of the slip angular frequency including the rotor equivalent resistance r_2 from the equation (23).

$$K_m = \frac{r_2}{\phi_{2a}} = \frac{1}{i_{1d} \cdot t_1} \ln\left(\frac{v_{ref}}{V_0}\right) \quad (23)$$

The block diagram for estimating rotor equivalent resistance r_2 is shown in Fig. 10.

The residual voltage after opening the motor terminal v_{1} and the reference voltage v_{ref} are constant, so that the logarithm calculation in equation (23) is calculated in advance and set.

Fig. 11 shows the experimental results of measuring some kinds of motors by this estimation system and the motors constants are as follows ;

- Rated voltages are 200 and 400v.
- Horse powers are from 1/4hp to 5hp.
- Constructions of motor are 2, 4 and 6 poles.

According to the above-mentioned conditions, rotator equivalent resistance r_2 is measured about the induction motor of a total of 36 types.

The difference between the estimated rotor resistance value and the one measured by the method obtained from no-load test and lock test is within $\pm$ 10%.

As a result, the rotor equivalent resistance r_2 of both rated voltage 200V series and 400V series of the induction motor are well coincidence and the measurement process of rotator equivalent resistance r_2 by the residual voltage of an induction motor is very effective.

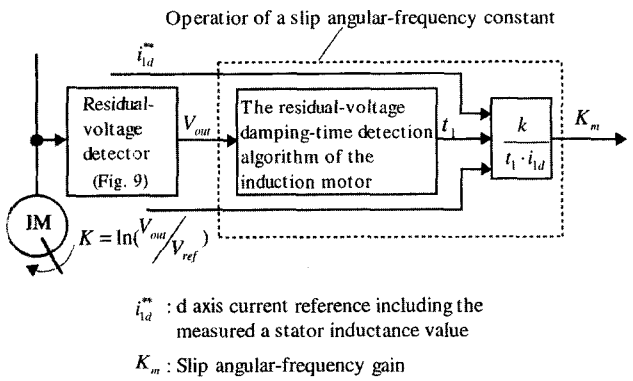

Fig. 10. Block diagram of rotor equivalent resistance detector of induction motor rotor.

4. Control System Configuration

Actual adjustable speed induction motor drive system with machine parameter measuring scheme is shown in Fig. 12. In addition to the vector control basic system of Fig. 2, automatic measurement system of the induction motor machine parameters is built into the system block diagram of Fig. 12.

The flowchart to estimate the stator and rotor circuit constants of the induction motor are shown in Fig. 13. In Fig. 12, the switch in the measurement section of stator winding resistance r_1 and stator winding inductance L_1 is the measurement loop used at the time of measurement of each induction motor constant, and shows that it is separated from an operation loop at the time of an after machine parameter measurement. Fig. 13 shows the flowchart of the algorithm which carries out the induction motor parameter automatic measurement of a vector control inverter system with the proposed motor machine parameter automatic measurement function to propose.

First, the frequency of the stator voltage is set to 0Hz, and stator winding resistance r_1 is measured. After measurement of the stator winding resistance r_1, the induction motor is rotated by predetermined angular frequency and stator winding inductance L_1 is measured.

Finally, the rotor equivalent resistance r_2 is measured from the residual-voltage wave which is observed at the power supply terminal after stopping the supply voltage to the induction motor, thus the measurement process of the induction motor machine parameter is completed.

The feasible system implementation is shown in Fig. 14. The power conversion processing of the inverter is based on the 3 phase-voltage-fed PWM inverter with IGBT bridge. 16-bit DSP (ADSP1201 product by Analog Devices) is used for the center of control. Special IC for 3 phase PWM signal generating of 8 bits resolution (upc15015, product by NEC) is used for generating PWM signal which frequency is 12 KHz. The A/D converter which has 12 bits resolution and 8 microseconds of conversion time are used for measuring the voltage between phases and the line current of the induction motor. The CT (DCS-150, product by TDK) in which the hall

effective element is built in is using sensing the current of the induction stator winding current.

In addition, the inverter system shown in Fig. 14 has I/O interface of the 7 segments LEDs for displaying the rotation frequency of the induction motor and also has the ten keyboards by which inverter drive data is input in.

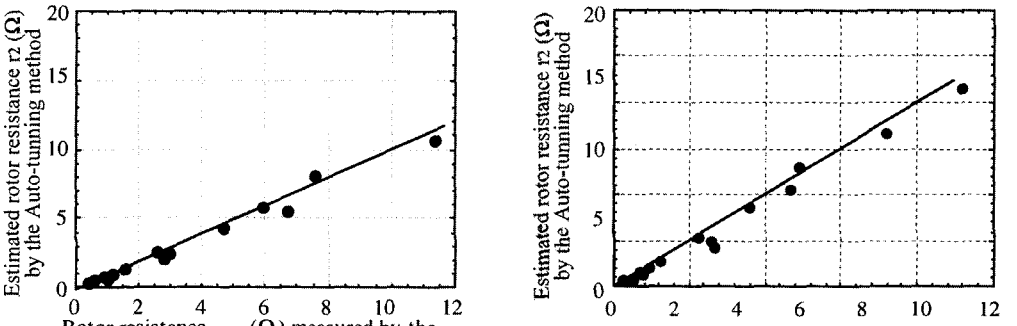

(a) Rotor Resistance of 200V rated Type Induction Motors

(b) Rotor Resistance of 400V rated Type Induction Motors

Fig. 11. Rotor resistance values estimated by digital signal processor incorporated into inverter.

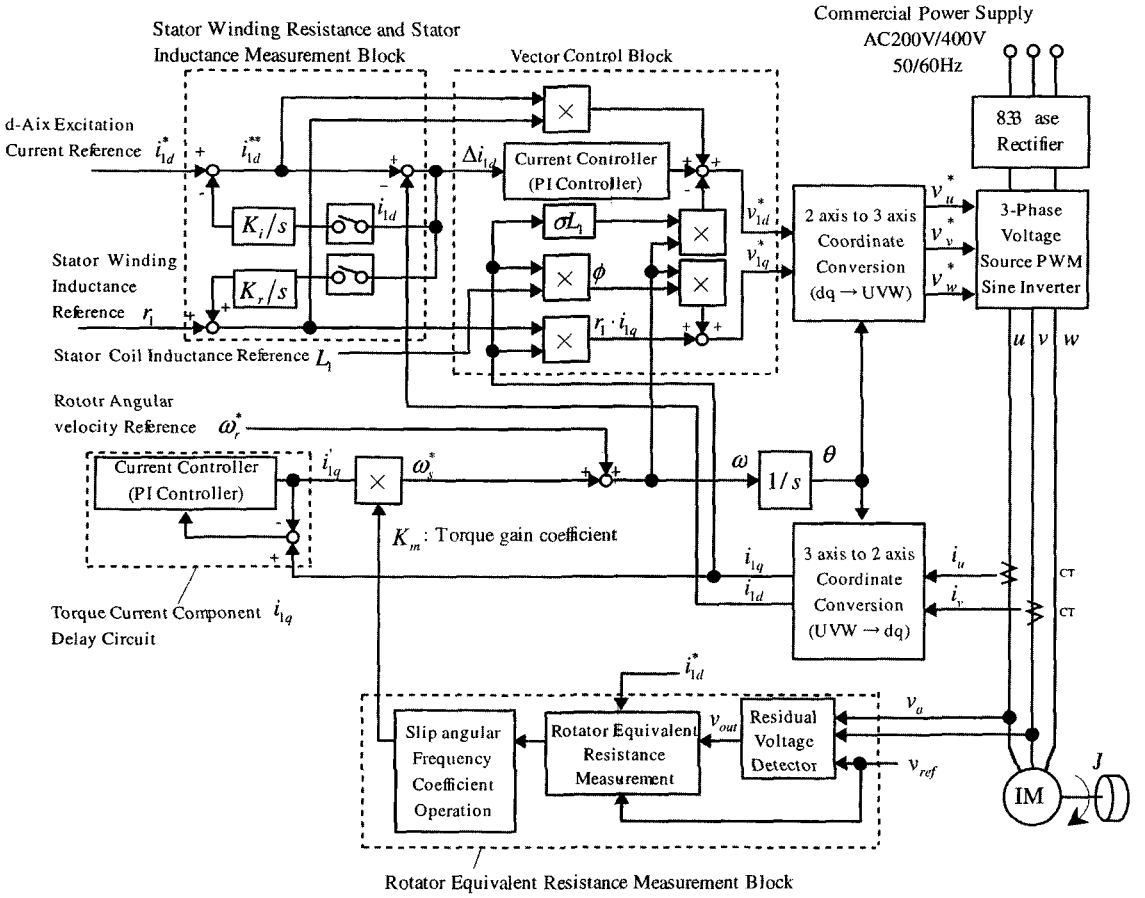

Fig. 12. Block diagram of control system with a novel auto-turning machine parameter estimation scheme.

The vector control software processing and the delay based software processing of torque current component can be achieved in term of DSP implementation and its peripheral circuits. In this case, the control procedures for the coordinate transformation and the reference voltage can be achieved within 100μsec . The machine parameter estimations and the delay based processing of torque current component in dynamic state can be performed during the sampling time T_s (=1ms). In this system, the current detection interface uses the isolated CT (current transformer) with hall-effect sensing device and 12 bit A/D converter.

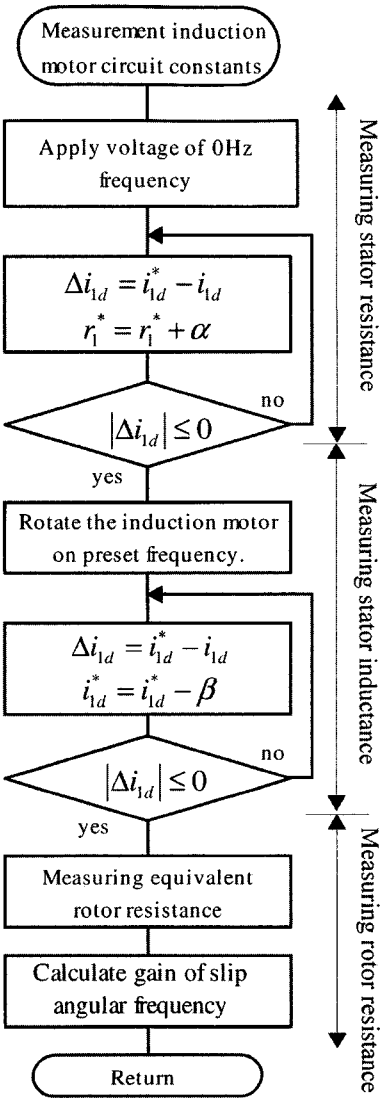

Fig. 13. Flowchart of machine parameter automatic estimation of the induction motor.

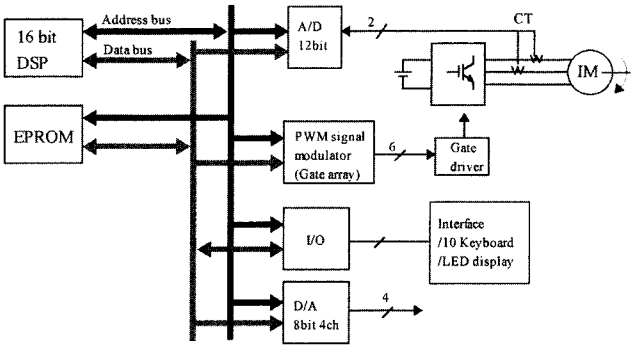

Fig. 14. Feasible DSP circuit implementation of vector controlled inverter.

5. Experimental Result and Their Practical Evalutions

Fig. 15 illustrates the dynamic speed transient response performance when step-rise load torque disturbance is applied to this induction motor drive system from no-load to full load torque. It is practically proven that the stator current of the induction motor drive system becomes stable without an excessive current in spite of largely changed load torque disturbances.

In addition to this, in experiment, the speed regulation factor in steady state is less than about 2.8% of the rated speed over wide ranges speed settings as well as large load torque disturbances. Furthermore, it is noted that the transient recovering time (settling time) is to be about 300msec.

Table.1 shows the machine constants measured by means of no-load test and lock test.

Table 1. Machine Parameters

Motor	r1(Ω)	r 2(Ω)	L1 (H)
Rated voltage :200V	2.50	2.47	0.15
Rated voltage :400V	1.54	1.97	0.11

Fig. 16 illustrates the steady state torque vs. speed characteristics of this motor speed control system. Note that the steady state accuracy of speed regulation for two induction motors is less than about 2% in a wide range of speed and load torque variation conditions.

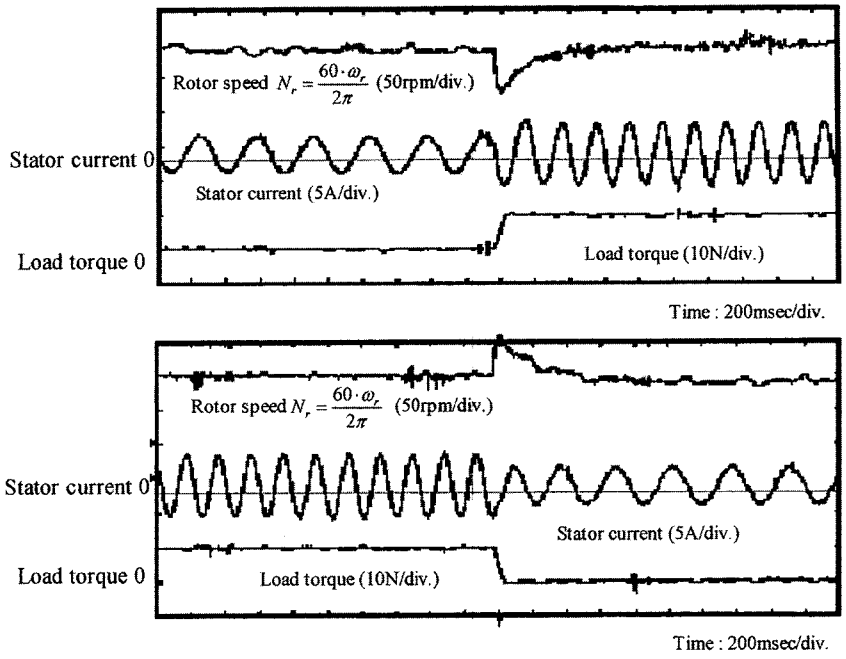

Fig. 15. Step speed response in case of load torque changed.

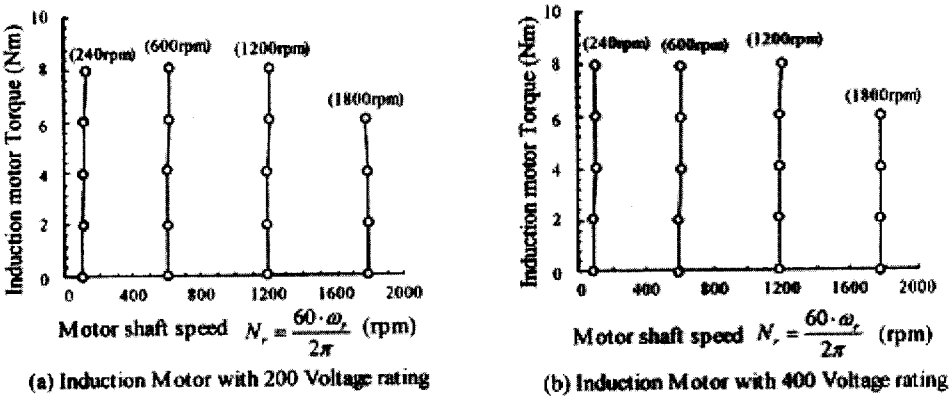

Fig. 16. Characteristics between motor speed and torque estimated by novel machine parameter auto-tuning method.

6. Conclusions

In this paper, the high performance and accuracy adjustable-speed induction motor drive system incorporating sensorless vector control based three-phase PWM IGBT inverter is demonstrated and characterized. This inverter has a novel automatic tuning machine operated circuit parameter estimation scheme in addition to the effective PI controller to delay the transient torque current component to reduce the excessive stator current in dynamic disturbances.

In this paper, the slip angular-frequency control system for speed sensorless vector controlling method of the induction motor and the proposed automatic parameter measuring method of a practical induction motor circuit were explained, the trial production experiment and the application experiment performed the property evaluation, and the validity was made clear from an experimental standpoint.

The inherent automatic tuning principle of the stator and rotor circuit parameters has been presented from theoretical and practical considerations.

The steady state variable speed regulation characteristics and dynamic speed response performances of this cost effective sensorless vector control inverter-fed have been illustrated and tested from experimental points of view.

The feature of this system is as follows.

(1) By measuring automatically stator winding resistance r_1, stator winding inductance L_1 and rotor equivalent resistance r_2 which are the induction motor equivalent circuit parameters, it proved that this novel sensorless vector control inverter is possible to control any kind of the induction motor at high-speed response and high precision speed control.

(2) The novel measuring method of the stator winding inductance L_1 is not the method of computing the inductance value itself directly but the method of operating the d-axis excitation current component on d-q 2-axis coordinates as a substitution value of stator winding inductance L_1.

(3) The system which measures the rotor equivalent resistance value r_2 was adopted from residual-voltage damping-time t_1 which is generated when the power supply terminal of the induction motor is opened under fixed rotation, as shown in Fig. 8.

Furthermore, microprocessor does not detect the residual-voltage damping-time t_1 directly, adapting the circuit using the comparator and the photo coupler, the rotor equivalent resistance r_2 will be possible to detect without microprocessor's burden.

Stator winding resistance r_1, stator winding inductance L_1 and the rotor equivalent resistance r_2 which are the parameters required in the sensorless vector control inverter system are able to be measured in short time and high accuracy, and the validity and practicality of novel measurement system were clarified.

References

[1] Toshiaki Okuyama, Noboru Fujimoto and Takayuki Matsui, "Vector Control Scheme of Induction Motor without Speed and Voltage Sensors", IEEJ Transaction on Industry Applications, Vol. 107, pp. 191~198, February 1987.

[2] Kouhei Ohnisi, Kunio Miyachi and Masayuki Terashima, "An Approach to Induction Motor Drive with Controlled Voltage Source", IEEJ Transaction on Power and Energy, pp. 25~30, Nov. 1984.

[3] Toshiaki Okuyama, Noboru Fujimoto and Hiroshi Fujii, "Simplified Vector Control System without Speed and Voltage Sensors–Effects of Setting Errors in Control Parameters and their Compensation–", IEEJ Transaction on Industry Applications, Vol. 110, pp. 477~486, May 1990.

[4] Naoki Ymamura, Masahiko Iwasaki and Hirotaka Sakurai, "PG-less Vector Control with Estimating Functions of Motor Parameter", IEEJ Transaction on Industry Applications, Vol. 107, No. 5, pp. 373~378, May 1991.

[5] Geng Yang and Tung-Hai Chin, "Hyperstability of the Full Oerder Adaptive Observer for Vector Controlled-Induction Motor Drive without Speed-Sensor", IEEJ Transaction on Industry Applications, Vol. 112, pp. 1047~1055, Nov. 1992.

[6] Tetsuo Kawamoto, Yukihiko Okamura, Yousuke Ishida and Hideaki Abe, "Blushless DC Motor for Massage Loungers", Proceeding of Small Motor International Conference 1993(SMIC'93), pp. 51~58, 1993.

[7] Yukihiko Okamura, Koji Soshin, Hiroaki Yuasa, Mutsuo Nakaoka and Eiji Hiraki, "High Performance Adjustable-Speed Induction Motor Drive System using Sensorless Vector Control-based PWM Inverter with Auto-Tuning Machine-Operated Estimation Scheme", IEE Japan RM, RM-94-62, pp. 21~30, July 1994.

[8] Yukihiko Okamura, Koji Soshin, Akihiro Yuasa and Yasuo Suzuki, "High Performance Adjustable-Speed Induction Motor Drive System using Sensorless Vector Controlled PWM Inverter with Auto-Tuning Machine-Operated Parameter Estimation Schemes", Proceedings Powersystems World Power Electronics and Conference, Intelligent Motion System, pp. 204~223, Sep. 1995.

[9] Yukihiko Okamura, Koji soshin, Akihiro Yuasa and Yasuo Suzuki, "High Performance Adjustable-Speed Induction Motor Drive System using Sensorless Vector Control-based PWM Inverter with Auto-Tuning Machine-Operated Parameter Estimation Schemes",

Proceeding of IEE-Korea International Conference on Power Electronics, pp. 804~809, Oct. 1995.

[10] Hideki Sugimoto, Li Ding and Masatoshi Koyasu, "An Identification Method of Primary and Secondary Resistance for Vector Controlled Induction Motor System", IEE Japan, Domestic Conference Transaction, pp. 997, March 1998.

[11] Kan Akatsu and Atsuo Kawamura, "On-line estimation of Speed and Secondary Resistance for the Speed Sensorless vector control of Induction Motor", IEE Japan, Domestic Conference Transaction pp. 899, March 1998.

[12] Mineo Tsuji, Katsuhiro Izumi and Eiji Yamada, "A Simplified Method of Vector-Controlled Induction Motor Drive System with Parameter Identification", IEEJ Transaction on Industry Applications Letter, Vol. 118D, pp. 1091~1092, Sep. 1998.

[13] Seiji Hashimoto, Hirohito Funato, Yutaka Imanari and Kenzo Kamiyama, "System Identification of Induction Motor for Auto Tuning-Design Method of Torque Control System using Identified Model", IEEJ Transaction on Industry Applications Letter, pp. 1241~1242, Oct. 2000.

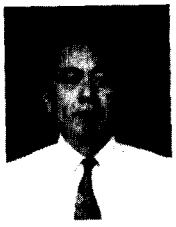

Koji Soshin received his M.Sc.-Eng from the Electronic Engineering Department, the Graduate School of Electrical and Electronics Engineering,. Kobe University, Kobe, Japan. He joined Matsushita Electric Works, Ltd. in 1979. He is interested in stepping motor applications, vector controlled inverter for the induction motor and power electronic circuits and systems technologies. He is now working in the power supplies for electric vehicle. He is now a Ph. D. candidate student in the Graduate School of Science and Engineering, Yamaguchi University, Yamaguchi, Japan. Mr. Soshin is a member of the Japan Society of Power Electronics.

Yukihiko Okamura received the B.Eng. degree in electrical engineering from Waseda University, Tokyo, Japan in 1984. Since his graduation, he has been with Research & Development Center of Matsushita Electric Works Ltd., Osaka, Japan in 1986. He is interested in stepping motor applications, vector controlled inverter for the induction motor and power electronic circuits and systems technologies. He is now working in the speed sensor-less control of the interior permanent magnet DC blush-less motor.

Tarek Ahmed received his M Sc.-Eng from the Electrical Engineering Department, Assiut University, Egypt in 1998. He is currently a Ph. D. candidate student in the Graduate School of Science and Engineering, the Power Electronic System and Control Engineering Laboratory at Yamaguchi University, Yamaguchi, Japan. His research interests are in the area of the new applications for the power electronic circuits and systems with the renewable energy and power systems and semiconductor power conditioners. Mr. Ahmed is a student-member of the IEEE and the Japan Society of the Power Electronics.

Mutsuo Nakaoka received his Dr-Eng. degree in Electrical Engineering from Osaka University, Osaka, Japan in 1981. He joined the Electrical and Electronics Engineering Department of Kobe University, Kobe, Japan in 1981. Since 1995, he has been a professor of the Electrical and Electronics Engineering Department, the Graduate School of Science and Engineering, Yamaguchi University, Yamaguchi, Japan. His research interests include application developments of power electronics circuit and systems. He received the 2001 premium paper award from IEE-UK and so on. Dr. Nakaoka is a member of the Institute of Electronics, Information and Communication Engineers of Japan, Institute of Illumination Engineering of Japan, European Power Electronics Association, the Japan Society of the Solar Energy, IEE-Korea and IEEE.